Siegert-state expansion for nonstationary systems. IV. Three-dimensional case

Oleg I. Tolstikhin
Russian Research Center, "Kurchatov Institute," Kurchatov Square 1, Moscow 123182, Russia
(Received 3 December 2007; published 17 March 2008)

The Siegert-state expansion approach [O. I. Tolstikhin, Phys. Rev. A **73**, 062705 (2006)] is extended to the three-dimensional case. Coupled equations defining the time evolution of coefficients in the expansion of the solution to the time-dependent Schrödinger equation in terms of partial-wave Siegert states are derived, and physical observables (probabilities of transitions to discrete states and the momentum distribution of ejected particles) are expressed in terms of these coefficients. The approach is implemented in terms of Siegert pseudostates and illustrated by calculations of the photodetachment of H^- by strong high-frequency laser pulses. The present calculations demonstrate that the interference effect in the laser-atom interaction dynamics found recently in the one-dimensional case [K. Toyota *et al.*, Phys. Rev. A **76**, 043418 (2007)] reveals itself in the three-dimensional case as well.

DOI: 10.1103/PhysRevA.77.032712 PACS number(s): 03.65.Nk, 31.15.−p, 34.10.+x, 32.80.Rm

I. INTRODUCTION

It is commonly known that transitions to the continuum are more difficult to treat than transitions between discrete states, in both stationary and nonstationary cases. In direct numerical grid approaches to the solution of the Schrödinger equation, the difficulties are caused by the finiteness of the box used in the calculations and artificial reflections at its boundaries. In close-coupling schemes resulting from basis-set expansion approaches, they are rooted in the fact that the continuum cannot be represented by a discrete square integrable basis. These difficulties may seem to be technical, but are in fact essential. They reflect a fundamental asymmetry of the standard formulation of scattering theory in which the discrete and continuous spectra are treated differently and the former is generally much easier to deal with than the latter.

The difficulties associated with the continuum may be resolved by reformulating scattering theory in terms of Siegert states (SSs). SSs are the eigenfunctions of the Hamiltonian which are regular in any finite part of configuration space and have only one type of waves, incoming or outgoing, in the asymptotic region. Such an eigenvalue problem was first considered by Siegert for *s*-wave scattering in a spherically symmetric finite range potential [1]. The main advantage of SSs is that they constitute a purely discrete (but not square integrable in the usual sense of the word) set. At the same time, they possess certain orthogonality and completeness properties, so that all major objects of scattering theory—bound and scattering states, Green's function, and scattering matrix—can be expressed in their terms. The program of reformulating scattering theory in terms of SSs became feasible a decade ago, with the introduction of Siegert pseudostates (SPSs) [2]. SPSs not only made the implementation of the theory of SSs in practical calculations possible, which is important for applications, but also provided a very simple algebraic approach using which the theory has been redeveloped and essentially extended [3–7]. These results have already found numerous applications in atomic physics [8–22].

The orthogonality and completeness properties of SSs qualify them as a basis suitable for expanding the continuum. The use of this basis opens the perspective to formulate a close-coupling approach in which the discrete and continuous spectra are treated on an equal footing. The development of such an approach in the nonstationary case was initiated in the first paper of the series [19]. The simplest nonstationary problem of *s*-wave motion in a time-dependent spherically symmetric potential was considered there. The solution to the time-dependent Schrödinger equation (TDSE) was sought as an expansion in terms of appropriate SSs. A set of coupled equations defining the coefficients was derived and physical observables were expressed in their terms. The coupled equations turned out to be pseudodifferential, which is the price for incorporating the continuum. The approach was implemented in terms of SPSs [3]. In the second paper [20], the approach was extended to a similar problem on the whole axis. This formulation was then applied to the analysis of a model one-dimensional (1D) laser-atom interaction problem [21]. The calculations reported in [19–21] have demonstrated that the SS expansion approach is free from the difficulties mentioned above and enables one to treat transitions to the continuum as easily as transitions between discrete states. The proposed numerical scheme is very accurate and capable of producing highly resolved spectra. In addition to these computational advantages, the SS expansion approach provides a theoretical framework for the analytical treatment of transitions to the continuum in adiabatic approximation. A first step in this direction has been made in the third paper of the series [22].

In the present paper, the SS expansion approach is extended to the 3D case. This became possible due to a recent generalization of the theory of SPS to nonzero angular momenta [7]. In Sec. II, we formulate the problem under consideration and, using the outgoing-wave boundary condition, present the TDSE in a matrix form suitable for the expansion in terms of SSs. In Sec. III, we define partial-wave SSs and derive coupled equations describing time evolution of the coefficients in the expansion of the solution to the TDSE in their terms. These equations have the same form as in the *s*-wave case [19], the only difference being that the SS basis now includes higher partial waves. We also express the observables—probabilities of transitions to discrete states and the momentum distribution of ejected particles—in terms of the solutions to the coupled equations. This com-

pletes the formulation of the method. The method is implemented in terms of SPSs [7]. In Sec. IV, it is illustrated by calculations of the photodetachment of H^- by strong high-frequency laser pulses. We focus on the same physical regime as considered in [21]. The present calculations show that the interference substructure of above-threshold ionization peaks found in the 1D case [21] appears in the 3D case as well. The evolution of this substructure with a variation of the parameters of the laser pulse is discussed. Section V concludes the paper.

II. BASIC EQUATIONS

A. Formulation of the problem

We consider a nonstationary system described by the TDSE (atomic units are used throughout the paper)

$$\left[i\frac{\partial}{\partial t} - H - U(\mathbf{r},t) \right] \psi(\mathbf{r},t) = 0, \tag{1}$$

where H is the Hamiltonian of an unperturbed spherically symmetric atomic system,

$$H = -\frac{1}{2}\frac{\partial^2}{\partial r^2} + \frac{\hat{\mathbf{l}}^2}{2r^2} + V(r), \tag{2}$$

and $U(\mathbf{r},t)$ represents an external field or some deformation of the atomic potential $V(r)$. Here $\psi(\mathbf{r},t)$ is the wave function multiplied by r and $\hat{\mathbf{l}}^2$ is the angular momentum operator squared. An important assumption is that both the time-independent $V(r)$ and time-dependent $U(\mathbf{r},t)$ potentials vanish beyond some finite radius,

$$V(r)|_{r\geq a} = U(\mathbf{r},t)|_{r\geq a} = 0, \tag{3}$$

or can be cut off without any appreciable effect on the observables. We also assume that

$$U(\mathbf{r},t)|_{t\to\pm\infty} = 0, \tag{4}$$

which, however, is not essential for the method; more general situations can be considered. The initial condition for Eq. (1) reads

$$\psi(\mathbf{r},t)|_{t\to-\infty} = \phi_0(\mathbf{r})e^{-iE_0t}, \tag{5}$$

where E_0 and $\phi_0(\mathbf{r})$ correspond to a bound state of H:

$$(H - E_0)\phi_0(\mathbf{r}) = 0, \tag{6a}$$

$$\phi_0(\mathbf{r})|_{r\to\infty} = 0, \quad \int_0^\infty dr \int |\phi_0(\mathbf{r})|^2 d\Omega = 1. \tag{6b}$$

Here and in the following we use the notation $\mathbf{r}=(r,\Omega)$, $\Omega=(\theta,\varphi)$, and $d\Omega=\sin\theta\, d\theta\, d\varphi$. The problem consists in calculating the distribution of probability to find the system in various bound and scattering states of H after the action of the external field is over.

B. Outgoing-wave boundary condition

Using the spherical symmetry of the unperturbed system, we seek the solution to Eq. (1) in the form of a partial-wave expansion:

$$\psi(\mathbf{r},t) = \sum_{lm} \psi_{lm}(r,t)Y_{lm}(\Omega). \tag{7}$$

Substituting this into Eq. (1), one obtains a set of coupled equations for the radial functions:

$$\left[i\frac{\partial}{\partial t} - H_l \right] \psi_{lm}(r,t) - \sum_{l'm'} U_{lm,l'm'}(r,t)\psi_{l'm'}(r,t) = 0, \tag{8}$$

where

$$H_l = -\frac{1}{2}\frac{d^2}{dr^2} + \frac{l(l+1)}{2r^2} + V(r) \tag{9}$$

and

$$U_{lm,l'm'}(r,t) = \int Y^*_{lm}(\Omega)U(\mathbf{r},t)Y_{l'm'}(\Omega)d\Omega. \tag{10}$$

The initial state is presented in the form

$$\phi_0(\mathbf{r}) = \phi_{l_0n_0}(r)Y_{l_0m_0}(\Omega). \tag{11}$$

Then the initial conditions for Eqs. (8) read

$$\psi_{lm}(r,t)|_{t\to-\infty} = \delta_{ll_0}\delta_{mm_0}\phi_{l_0n_0}(r)e^{-iE_0t}. \tag{12}$$

Let us discuss the boundary conditions for Eqs. (8).

The functions $\psi_{lm}(r,t)$ satisfy the regularity boundary condition at $r=0$:

$$\psi_{lm}(0,t) = 0. \tag{13}$$

They also satisfy certain boundary condition at $r=a$. To formulate it, we need to recall some notation introduced in [19]. The function and derivative value operators at $r=a$ are

$$\mathcal{F} = \delta(r-a), \quad \mathcal{D} = \delta(r-a)\frac{d}{dr}. \tag{14}$$

A pseudodifferential operator $\hat{\lambda}_t$ acts on functions of time representable in the form

$$f(t) = \int_{-\infty}^{\infty} f(E)e^{-iEt}\frac{dE}{2\pi} \tag{15}$$

and is defined by

$$\hat{\lambda}_t f(t) = \int_{-\infty}^{\infty} ikf(E)e^{-iEt}\frac{dE}{2\pi} \tag{16a}$$

$$= \frac{2e^{3i\pi/4}}{\sqrt{2\pi}}\frac{d}{dt}\int_{-\infty}^{t}\frac{f(t')}{(t-t')^{1/2}}dt'. \tag{16b}$$

In this paper, E and k always denote energy and momentum related to each other by

$$E = k^2/2, \quad k = \sqrt{2E}, \tag{17}$$

where the branch of the square root function for which $\mathrm{Im}\, k>0$ on the physical sheet of E is meant. As usual in scattering theory [23], it is understood that the integration path in Fourier integrals of the type (15) and (16a) lies on the physical sheet infinitesimally above the real axis. The opera-

tor $(\hat{\lambda}_t - iq)^{-1}$ for $\pi/2 \le \arg q \le 2\pi$ is defined by

$$(\hat{\lambda}_t - iq)^{-1} f(t) = -i \int_{-\infty}^{\infty} \frac{f(E) e^{-iEt}}{k-q} \frac{dE}{2\pi} \tag{18a}$$

$$= \int_{-\infty}^{t} g(t-t';q) f(t') dt', \tag{18b}$$

where $g(t;q)$ is the retarded Green's function for the reciprocal operator $(\hat{\lambda}_t - iq)$:

$$(\hat{\lambda}_t - iq) g(t;q) = \delta(t), \quad g(t;q)|_{t<0} = 0. \tag{19}$$

This function can be expressed in terms of the Faddeeva function $w(z)$ [see Eqs. (7.1.4) and (7.1.11) in [24]]:

$$g(t;q) = \theta(t) \left[\frac{e^{-3i\pi/4}}{\sqrt{2\pi t}} - \frac{q}{2} w(-e^{i\pi/4} q \sqrt{t/2}) \right]. \tag{20}$$

Using the fact that $w(z)$ is an entire function, via the analytic continuation in q, Eqs. (18b) and (20) are valid for any complex q. For a more detailed discussion of $\hat{\lambda}_t$ and related operators see the Appendixes in [19,22].

Taking into account Eqs. (3), the potential energy terms in Eqs. (8) vanish in the outer region $r \ge a$. The resulting uncoupled free equations can be solved by the Fourier transformation in time. Following the argumentation of [19], it can be shown that for the solutions satisfying initial conditions (12) the Fourier transform of $\psi_{lm}(r,t)$ at energy E may have only outgoing (this term includes truly outgoing, for $E>0$, and exponentially decaying, for $E<0$) waves in the asymptotic region. Thus one obtains

$$\psi_{lm}(r,t) = \int_{-\infty}^{\infty} c_{lm}(E) e_l(kr) e^{-iEt} \frac{dE}{2\pi}, \quad r \ge a, \tag{21}$$

where $e_l(z) = i^{l+1} z h_l^{(1)}(z)$ and $h_l^{(1)}(z)$ is a spherical Hankel function of the first kind [24]. For our purposes, it is more convenient to use another representation for $e_l(z)$ [7]:

$$e_l(z) = \frac{\theta_l(-iz) e^{iz}}{(-iz)^l}, \quad \theta_l(z) = \prod_{p=1}^{l} (z - z_{lp}), \tag{22}$$

where $\theta_l(z)$ is the reverse Bessel polynomial of order l and z_{lp}, $p=1,\ldots,l$, are its zeros [25]. The function $e_l(kr)$ satisfies $e_l(kr)|_{r\to\infty} = e^{ikr}$. More specifically, we have

$$\frac{\partial e_l(kr)}{\partial r} = \left[ik - \frac{1}{r} \sum_{p=1}^{l} \frac{z_{lp}}{ikr + z_{lp}} \right] e_l(kr), \tag{23}$$

which is the outgoing-wave boundary condition in the energy domain. Introducing the notation

$$\tilde{\psi}_{lm}(r,t) = \hat{\lambda}_t \psi_{lm}(r,t), \tag{24a}$$

$$\psi_{lmp}(t) = -\frac{z_{lp}}{a} (\hat{\lambda}_t + z_{lp}/a)^{-1} \psi_{lm}(a,t), \quad p = 1, \ldots, l, \tag{24b}$$

from Eqs. (21) and (23) we obtain

$$\mathcal{D}\psi_{lm}(r,t) = \mathcal{F} \left[\tilde{\psi}_{lm}(r,t) + \frac{1}{a} \sum_{p=1}^{l} \psi_{lmp}(t) \right]. \tag{25}$$

This is the boundary condition mentioned above. It has the meaning of the outgoing-wave boundary condition in the time domain and generalizes a similar condition given in [19,26] to nonzero angular momenta. This condition enables one to eliminate the outer region $r>a$ from the consideration and plays an important role in the present approach.

C. Matrix form of the time-dependent Schrödinger equation

Let $\mathbb{H}$ denote a space of functions $u(r)$ defined in the interval $0 \le r \le a$ and satisfying

$$u(0) = 0, \quad u(a) < \infty, \quad \int_0^a u^2(r) dr < \infty. \tag{26}$$

We also introduce an extended space

$$\mathbb{H}^{(l)} = \mathbb{H} \oplus \mathbb{H} \oplus \mathbb{C}^l, \tag{27}$$

where $\mathbb{C}^l$ is the l-dimensional complex vector space. The elements of $\mathbb{H}^{(l)}$ are vectors of the form

$$\boldsymbol{u}(r) = \begin{pmatrix} u(r) \\ \tilde{u}(r) \\ u_1 \\ \cdots \\ u_l \end{pmatrix}, \tag{28}$$

where $u(r)$ and $\tilde{u}(r)$ belong to $\mathbb{H}$ and u_p, $p=1,\ldots,l$, are complex numbers. The inner product in $\mathbb{H}^{(l)}$ is defined by

$$\langle \boldsymbol{u}(r) | \boldsymbol{v}(r) \rangle_l = \int_0^a [u(r) v(r) + \tilde{u}(r) \tilde{v}(r)] dr + \sum_{p=1}^{l} u_p v_p. \tag{29}$$

Note that there is no complex conjugation in this formula.

Let us join the function $\psi_{lm}(r,t)$ and its derivatives defined by Eqs. (24) in a vector:

$$\boldsymbol{\psi}_{lm}(r,t) = \begin{pmatrix} \psi_{lm}(r,t) \\ \tilde{\psi}_{lm}(r,t) \\ \psi_{lm1}(t) \\ \cdots \\ \psi_{lml}(t) \end{pmatrix}. \tag{30}$$

The functions $\psi_{lm}(r,t)$ and $\tilde{\psi}_{lm}(r,t)$ belong to $\mathbb{H}$; therefore, the vector $\psi_{lm}(r,t)$ belongs to $\mathbb{H}^{(l)}$. We introduce a square $(2+l)\times(2+l)$ matrix operator

$$\Lambda_l = \begin{pmatrix} 0 & 1 & 0 & 0 & \cdots & 0 \\ -2\tilde{H}_l & \mathcal{F} & \mathcal{F}/a & \mathcal{F}/a & \cdots & \mathcal{F}/a \\ -z_{l1}\mathcal{F}^T/a & 0 & -z_{l1}/a & 0 & \cdots & 0 \\ -z_{l2}\mathcal{F}^T/a & 0 & 0 & -z_{l2}/a & \cdots & 0 \\ \hdashline -z_{ll}\mathcal{F}^T/a & 0 & 0 & 0 & \cdots & -z_{ll}/a \end{pmatrix}, \tag{31}$$

where $\mathcal{F}^T$ is an operator acting on functions from $\mathbb{H}$ according to (in a sense, $\mathcal{F}^T$ is a transpose of $\mathcal{F}$, which explains the notation)

$$\mathcal{F}^T u(r) = u(a), \tag{32}$$

and $\tilde{H}_l$ is the Hermitized partial-wave Hamiltonian defined by

$$\tilde{H}_l = H_l + \frac{1}{2}\mathcal{D}. \tag{33}$$

We also introduce a rectangular $(2+l)\times(2+l')$ matrix function

$$\mathbf{U}_{lm,l'm'}(t) = \begin{pmatrix} 0 & 0 & \cdots & 0 \\ U_{lm,l'm'}(r,t) & 0 & \cdots & 0 \\ 0 & 0 & \cdots & 0 \\ \hdashline 0 & 0 & \cdots & 0 \end{pmatrix}, \tag{34}$$

where all elements but one are zero. Then, using Eqs. (24a), (24b), and (25), Eqs. (8) can be presented in the form

$$[\hat{\lambda}_t - \mathbf{\Lambda}_l]\boldsymbol{\psi}_{lm}(r,t) + 2\sum_{l'm'} \mathbf{U}_{lm,l'm'}(t)\boldsymbol{\psi}_{l'm'}(r,t) = 0. \tag{35}$$

These equations are equivalent to Eqs. (8) for the solutions satisfying the outgoing-wave boundary condition (25). Now we make a crucial step: we shall treat the components of $\boldsymbol{\psi}_{lm}(r,t)$ [see Eq. (30)] as independent unknowns defined by Eqs. (35), which implies an extension of the original Hilbert space. This generalizes a similar construction introduced in [19] to the 3D case. We call Eqs. (35) the matrix form of the TDSE (the term "matrix" refers to the extension of the Hilbert space, not to the partial-wave expansion). Presenting the TDSE in such a form opens the way for the expansion of the solution in terms of SSs.

III. EXPANSION IN TERMS OF SIEGERT STATES

A. Partial-wave Siegert states

The theory of SPSs for nonzero angular momenta was developed in [7]; corresponding results for SSs follow in the limit $N\to\infty$, where N is the dimension of a primitive radial basis defining the SPSs. We here summarize the basic relations needed for the following, reformulating them in the present notation. The partial-wave SSs are defined by [7]

$$(H_l - E)\phi(r) = 0, \tag{36a}$$

$$\phi(0) = 0, \tag{36b}$$

$$\left(\frac{d}{dr} - ik + \frac{1}{a}\sum_{p=1}^{l}\frac{z_{lp}}{ika + z_{lp}}\right)\phi(r)\bigg|_{r=a} = 0. \tag{36c}$$

The solutions to this eigenvalue problem will be denoted by k_{ln}, $E_{ln}=k_{ln}^2/2$, and $\phi_{ln}(r)$. Similarly to Eqs. (24a), (24b), and (30), we introduce the notation

$$\tilde{\phi}_{ln}(r) = ik_{ln}\phi_{ln}(r), \tag{37a}$$

$$\phi_{lnp} = -\frac{z_{lp}\phi_{ln}(a)}{ik_{ln}a + z_{lp}}, \quad p = 1, \ldots, l, \tag{37b}$$

and

$$\boldsymbol{\phi}_{ln}(r) = \begin{pmatrix} \phi_{ln}(r) \\ \tilde{\phi}_{ln}(r) \\ \phi_{ln1} \\ \cdots \\ \phi_{lnl} \end{pmatrix}. \tag{38}$$

The functions $\phi_{ln}(r)$ and $\tilde{\phi}_{ln}(r)$ belong to $\mathbb{H}$; hence, the vector $\boldsymbol{\phi}_{ln}(r)$ belongs to $\mathbb{H}^{(l)}$. Using Eqs. (36c), (37a), and (37b), Eq. (36a) can be presented in a matrix form similar to Eq. (35):

$$[\mathbf{\Lambda}_l - ik_{ln}]\boldsymbol{\phi}_{ln}(r) = 0. \tag{39}$$

The solutions to this equation—i.e., the vectors (38)—will be also called SSs. They are orthogonal with respect to the inner product [7]

$$\langle \boldsymbol{\phi}_{ln}(r)|\mathbf{W}_l\boldsymbol{\phi}_{ln'}(r)\rangle_l = 2ik_{ln}\delta_{nn'}, \tag{40}$$

where the $(2+l)\times(2+l)$ weight matrix $\mathbf{W}_l$ is given by

$$\mathbf{W}_l = \begin{pmatrix} -\mathcal{F} & 1 & 0 & 0 & \cdots & 0 \\ 1 & 0 & 0 & 0 & \cdots & 0 \\ 0 & 0 & -1/z_{l1} & 0 & \cdots & 0 \\ 0 & 0 & 0 & -1/z_{l2} & \cdots & 0 \\ \hdashline 0 & 0 & 0 & 0 & \cdots & -1/z_{ll} \end{pmatrix}. \tag{41}$$

They form a complete set in $\mathbb{H}^{(l)}$, which fact is expressed by [7]

$$\sum_n \frac{1}{2ik_{ln}}\boldsymbol{\phi}_{ln}(r)\boldsymbol{\phi}_{ln}^T(r') = \delta(r-r')\mathbf{W}_l^{-1}, \tag{42}$$

where T stands for transpose and

$$\mathbf{W}_l^{-1} = \begin{pmatrix} 0 & 1 & 0 & 0 & \cdots & 0 \\ 1 & \mathcal{F} & 0 & 0 & \cdots & 0 \\ 0 & 0 & -z_{l1} & 0 & \cdots & 0 \\ 0 & 0 & 0 & -z_{l2} & \cdots & 0 \\ \hdashline 0 & 0 & 0 & 0 & \cdots & -z_{ll} \end{pmatrix}. \tag{43}$$

The orthogonality (40) and completeness (42) relations express the most essential for applications properties of partial-wave SSs. Many other useful relations can be found in [7].

B. Expansion in the inner region: Coupled equations for the coefficients

The solutions to Eq. (35) in the inner region can be sought in the form

$$\psi_{lm}(r,t) = \sum_n a_\nu(t)\phi_{ln}(r), \quad 0 \le r \le a. \tag{44}$$

We have introduced here a multi-index ν enumerating partial-wave SSs including the angular factor $Y_{lm}(\Omega)$:

$$\nu = (l,m,n). \tag{45}$$

Similarly, we shall write $\nu' = (l',m',n')$; the initial state in Eqs. (5) and (12) will be indicated by $\nu=0$. Substituting Eq. (44) into Eq. (35) and using Eq. (40), we obtain a set of coupled pseudodifferential equations defining the coefficients $a_\nu(t)$:

$$ik_{ln}(\hat{\lambda}_t - ik_{ln})a_\nu(t) + \sum_{\nu'} U_{\nu\nu'}(t)a_{\nu'}(t) = 0, \tag{46a}$$

$$a_\nu(t)|_{t\to-\infty} = \delta_{\nu 0}e^{-iE_0 t}, \tag{46b}$$

where

$$U_{\nu\nu'}(t) = \langle \phi_{ln}(r)|\mathbf{W}_l\mathbf{U}_{lm,l'm'}(t)\phi_{l'n'}(r)\rangle_l = \int_0^a \phi_{ln}(r)U_{lm,l'm'}(r,t)\phi_{l'n'}dr. \tag{47}$$

Using the Green's function for the operator $(\hat{\lambda}_t - iq)$ [see Eqs. (19) and (20)], we can rewrite Eqs. (46a) in an integral form

$$a_\nu(t) = \delta_{\nu 0}e^{-iE_0 t} + \frac{i}{k_{ln}}\sum_{\nu'}\int_{-\infty}^{t} g(t-t';k_{ln})U_{\nu\nu'}(t')a_{\nu'}(t')dt', \tag{48}$$

which incorporates the initial condition (46b).

Equations (46) and (48) are the main result in the formulation of the present approach. Remarkably, they have the same form as the corresponding equations in the s-wave [19] and 1D [20] cases, the only difference being in the set of SSs used in the expansion (44). This implies that upon appropriate generalization of SSs these equations may apply to more general physical situations. These equations are not what one is well familiar with in atomic physics. Some general mathematical results on equations of this type can be found in fractional calculus [27–29]. However, only primitive cases—e.g., equations with constant coefficients—are treated there. Some useful experience has been accumulated in [19–22]. In particular, an algorithm for the numerical solution of such equations was proposed [19] and a procedure to construct their asymptotic solution in adiabatic approximation was developed [22]. It is clear that the efficiency of the present approach depends on the availability of efficient mathematical techniques to work with Eqs. (46) and (48), so further progress in this direction is desirable.

C. Wave function in the outer region

In the outer region $r \ge a$ the function $\psi_{lm}(r,t)$ is given by Eq. (21). Setting $r=a$ in this equation, we find

$$c_{lm}(E) = \frac{1}{e_l(ka)}\int_{-\infty}^{\infty}\psi_{lm}(a,t)e^{iEt}dt. \tag{49}$$

On the other hand, requiring continuity of $\psi_{lm}(r,t)$ at $r=a$, from Eq. (44) we have

$$\psi_{lm}(a,t) = \sum_n a_\nu(t)\phi_{ln}(a). \tag{50}$$

Equations (21), (49), and (50) express $\psi_{lm}(r,t)$ for $r \ge a$ in terms of the coefficients $a_\nu(t)$. Thus the solutions to Eqs. (8) in the whole interval $0 \le r < \infty$, and hence the complete wave function, are expressed in terms of the solutions to the coupled equations (46) and (48).

D. Observables

It remains to express physical observables in terms of the coefficients $a_\nu(t)$. This is not a straightforward task because these coefficients do not have the usual meaning of amplitudes of probability. Indeed, we recall that SSs are not even normalizable in the usual sense of the word. A more careful consideration is needed.

Let $\{b\}_l$ denote the set of multi-indices ν corresponding to bound SSs with angular momentum l and $\{b\}$ be the collection of such sets for all values of l. Let $\varphi_{ln}(r)$ and $\varphi_l(r,k)$ denote bound and scattering states of H_l. The latter functions are normalized according to

$$\varphi_l(r,k)|_{r\to\infty} = e^{-ikr} - (-1)^l S_l(k)e^{ikr}, \tag{51}$$

where $S_l(k)$ is the partial-wave scattering matrix for the potential $V(r)$ (we use the same notation as in [7]). Then, taking into account Eq. (4), the large time asymptotics of $\psi_{lm}(r,t)$ has the form

$$\psi_{lm}(r,t)|_{t\to\infty} = \sum_{n\in\{b\}_l} C_\nu\varphi_{ln}(r)e^{-iE_{ln}t} + \int_0^\infty C_{lm}(k)\varphi_l(r,k)e^{-iEt}\frac{dk}{2\pi}. \tag{52}$$

All the observables can be expressed in terms of the coefficients C_ν and $C_{lm}(k)$ in this expansion; thus, the problem consists in expressing these coefficients in terms of $a_\nu(t)$. The derivation is similar to that in [19], so we skip the details here. From Eqs. (48), using the asymptotics of $g(t;q)$ for $t \to \infty$ [19], we obtain

$$a_\nu(t)|_{t\to\infty} = \begin{cases} a_\nu e^{-iE_{ln}t}, & \nu \in \{b\}, \\ O(t^{-3/2}), & \nu \notin \{b\}. \end{cases} \tag{53}$$

It can be shown that the bound-state amplitude is given by

$$C_\nu = a_\nu, \quad \nu \in \{b\}. \tag{54}$$

It can be also shown that the scattering-state amplitude is given by

$$C_{lm}(k) = (-1)^{l+1}kS_l^*(k)c_{lm}(E), \tag{55}$$

where $c_{lm}(E)$ is the coefficient in Eq. (21) which is given in terms of $a_\nu(t)$ by Eqs. (49) and (50). In principle, these for-

mulas solve the problem formulated above. However, for the numerical treatment it is more convenient to express the observables in terms of the functions

$$A_\nu(E) = \sum_{\nu'} \int_{-\infty}^{\infty} U_{\nu\nu'}(t) a_{\nu'}(t) e^{iEt} dt. \tag{56}$$

To calculate these functions, one needs to know $a_\nu(t)$ only within a finite interval where $U_{\nu\nu'}(t)$ differs from zero. This information is directly provided by the solution of Eq. (46a) and (46b) or (48). Let us summarize the final formulas to be used in the calculations. The probability to find the system in a bound state after the action of the external field is over is given by

$$P_\nu \equiv |C_\nu|^2 = |\delta_{\nu 0} - iA_\nu(E_{ln})|^2, \quad \nu \in \{b\}. \tag{57}$$

The momentum distribution of ejected particles in a partial wave is

$$P_{lm}(k) \equiv |C_{lm}(k)|^2 = \left| \frac{k}{e_l(ka)} \sum_n \frac{A_\nu(E)\phi_{ln}(a)}{k_{ln}(k-k_{ln})} \right|^2. \tag{58}$$

The 3D momentum distribution of ejected particles is

$$P(\mathbf{k}) \equiv \frac{1}{2\pi} \left| \sum_{lm} c_{lm}(E) Y_{lm}(\Omega) \right|^2 = \frac{1}{2\pi} \left| \sum_{\nu} \frac{A_\nu(E)\phi_{ln}(a) Y_{lm}(\Omega)}{e_l(ka) k_{ln}(k-k_{ln})} \right|^2, \tag{59}$$

where $\mathbf{k} = (k, \Omega)$. These formulas complete the formulation of the present approach. For consistency of the presentation, we give expressions for several other characteristics of transitions to the continuum in terms of the momentum distributions, simultaneously introducing our notation. The energy distribution and the probability of transitions to the continuum in a partial wave are

$$P_{lm}(E) = \frac{P_{lm}(k)}{2\pi k}, \quad P_{lm}^{(c)} = \int_0^\infty P_{lm}(E) dE. \tag{60}$$

The total energy distribution of ejected particles is

$$P(E) = \sum_{lm} P_{lm}(E) = k \int P(\mathbf{k}) d\Omega. \tag{61}$$

The total probability of transitions to the continuum is

$$P_c = \sum_{lm} P_{lm}^{(c)} = \int_0^\infty P(E) dE = \int P(\mathbf{k}) d^3\mathbf{k}. \tag{62}$$

Finally, the unitarity condition reads

$$\sum_{\nu \in \{b\}} P_\nu + P_c = 1. \tag{63}$$

IV. ILLUSTRATIVE CALCULATIONS: PHOTODETACHMENT OF H^-

One of the most interesting applications of the present approach is the study of the interaction of strong laser pulses with atomic and molecular systems. The Coulomb tail of the atomic potential $V(r)$ and the divergence of the dipole laser-atom interaction potential $U(\mathbf{r},t)$ at large r violate conditions (3), so the approach is not directly applicable to, say, the hydrogen atom. However, there are systems for which conditions (3) are fulfilled. For example, a heteronuclear diatomic molecule interacting with a laser field is described by Eq. (1) in situations when the electronic degrees of freedom can be separated out in the Born-Oppenheimer approximation. Both the interatomic potential $V(r)$ and the laser-molecule interaction potential $U(\mathbf{r},t)$, which is proportional to the molecular dipole moment, rapidly vanish at large separations between the atoms, provided that the molecule dissociates into two neutral fragments. Such a system in the s-wave case was considered in [22]. Another example is the interaction of a negative atomic ion with a laser field considered in the one-electron approximation in the Kramers-Henneberger (KH) frame [30,31]. This problem can be also treated by the present approach. Such a system in the 1D case was considered in [21]. The present formulation enables one to extend the analysis of [21,22] to the 3D case.

A. Model

We illustrate the method by calculations of the photodetachment of H^- by strong high-frequency linearly polarized laser pulses. The ion H^- is often described by a zero-range potential [32,33]. Several more realistic one-electron potentials are also in use [34–37]. We adopt the following simple model for the time-independent potential:

$$V(r) = -V_0 \exp(-r^2/r_0^2), \tag{64}$$

where $V_0 = 0.383\ 108\ 7$ and $r_0 = 2.5026$. These parameters are chosen to obtain only one bound state with energy $E_0 = -0.027\ 751\ 0$ and s-wave scattering length equal to 5.965, in full agreement with accurate variational results for H^- [38,39]. The z axis of the coordinate system is directed along the direction of polarization, so the electric field in the laser pulse is $F(t)\mathbf{e}_z$. We consider the problem in the KH frame [30,31]. Then the time-dependent potential is given by

$$U(\mathbf{r},t) = V(|\mathbf{r} + z(t)\mathbf{e}_z|) - V(r), \tag{65}$$

where $z(t)$ is a classical trajectory of the electron in the laser field defined by

$$\ddot{z}(t) = -F(t), \tag{66a}$$

$$z(t)|_{t\to-\infty} = \dot{z}(t)|_{t\to-\infty} = 0. \tag{66b}$$

We consider pulses of finite duration having the shape

$$F(t) = F_0 \sin^2(\pi t/T)\cos\,\omega t, \quad 0 \le t \le T, \tag{67}$$

where the number of optical cycles per pulse, $n_{oc} = \omega T/2\pi$, is an integer. In this case $z(T) = \dot{z}(T) = 0$, the wave function in the KH frame for $t \ge T$ coincides (up to a constant phase factor) with that in the laboratory frame, and hence observables also coincide [21]. This means that observables can be calculated in the KH frame using formulas given in Sec. III D; in a more general case, if $z(T) \neq 0$ or $\dot{z}(T) \neq 0$, an ad-

ditional transformation from the KH to laboratory frame is needed. The dynamics of the photodetachment process crucially depends on the amplitude F_0, frequency ω, and duration $T=n_{oc}(2\pi/\omega)$ of the laser pulse. We concentrate on one particular physical regime favorable for the observation of the interference effect discussed in [21]. This regime is characterized by high frequencies $\omega \gg |E_0|$ and sufficiently strong fields F_0, so that the amplitude of classical oscillations of the electron in the laser field $\alpha=F_0/\omega^2$ is larger than the size of the initial state and stabilization against photodetachment occurs [40,41]. Let us define a reference laser pulse in this regime: $F_0=0.5$ ($I=cF_0^2/8\pi=8.8\times10^{15}$ W/cm^2), $\omega=\pi/10$ (8.55 eV), and $T=500$ (12.1 fs); hence, $n_{oc}=25$ and $\alpha=50/\pi^2\approx5.1$. We present calculations for several pulses in this range of the parameters.

B. Implementation

The initial state in the present system corresponds to $l_0=m_0=0$; see Eq. (12). The magnetic quantum number m is conserved in the case of linear polarization, so one should set $m=0$ and omit summations in m in the above formulation. The approach is implemented in terms of SPSs [7]. The partial-wave SPSs with the angular momentum l are constructed using a discrete variable representation (DVR) [42–44] based on the Jacobi polynomials $P_n^{(0,2l)}(x)$. Let N be the dimension of the DVR basis (we use the same N for all values of l) and L be the maximum angular momentum retained in the partial-wave expansion (7). Then the number of coupled equations (46a) is $(L+1)(4N+L)/2$. We solve these equations in the integral form (48) using an algorithm described in [19]. The convergence in terms of the time step is controlled by how well the unitarity condition (63) is satisfied. This part of the numerical procedure is essentially the same as that used in [19–22]. Analysis of convergence of the SPS expansions for scattering characteristics of the time-independent potential (64) shows that it can be safely cut off at $r=6$. The classical trajectory defined by Eqs. (66a), (66b), and (67) satisfies $|z(t)|\leq\alpha$; hence, the time-dependent potential (65) can be cut off at $r=6+\alpha$. We emphasize that only this very limited region of space is to be considered in the present approach, independently of the duration of the pulse. The results reported below are obtained with the cutoff radius $a=12$, the number of DVR basis functions $N=40$, maximum angular momentum $L=10$, and time step 0.1 and are converged with respect to all these parameters. The convergence of the partial-wave expansion is illustrated in Table I.

C. Results

There is only one bound state in the system, so we discuss only transitions to the continuum—that is, photodetachment. We start with the reference laser pulse with $F_0=0.5$, $\omega=\pi/10$, and $T=500$. The total and several lowest partial-wave energy distributions of photodetached electrons are shown in Fig. 1. One can clearly see a sequence of above-threshold ionization (ATI) peaks [45] located near multiphoton absorption energies. In partial-wave spectra with even (odd) angular momentum l, even (odd) ATI peaks are more pronounced, which is a manifestation of the dipole selection rule. The height of ATI peaks in the total spectrum monotonically decreases as the order of the peak grows. In general, this spectrum looks similar to that calculated for similar laser parameters ($F_0=0.5$, $\omega=\pi/10$, and $T=2000$) in the 1D case [21]. The corresponding partial-wave and total photodetachment probabilities are listed in Table I. One can see that the partial-wave expansion rapidly converges in the present case. Similar calculations with $L=5$ and 8 give $P_5^{(c)}=0.104\times10^{-2}$ and $P_8^{(c)}=0.137\times10^{-4}$, respectively, without changing P_c within the specified accuracy. The total photodetachment probability P_c is close to unity, so the present situation is very far from the perturbative regime. The 3D momentum distribution of ejected electrons for the same laser pulse is shown in Fig. 2. In the case of linear polarization the func-

TABLE I. Partial-wave $P_l^{(c)}$ and total $P_c=\Sigma_l P_l^{(c)}$ photodetachment probabilities for the reference laser pulse (same as in Figs. 1 and 2). $a[b]$ means $a\times10^b$.

l	Probability	l	Probability
0	0.169	6	0.341[−3]
1	0.705	7	0.623[−4]
2	0.322[−1]	8	0.149[−4]
3	0.363[−1]	9	0.290[−5]
4	0.324[−2]	10	0.575[−6]
5	0.114[−2]	total	0.947

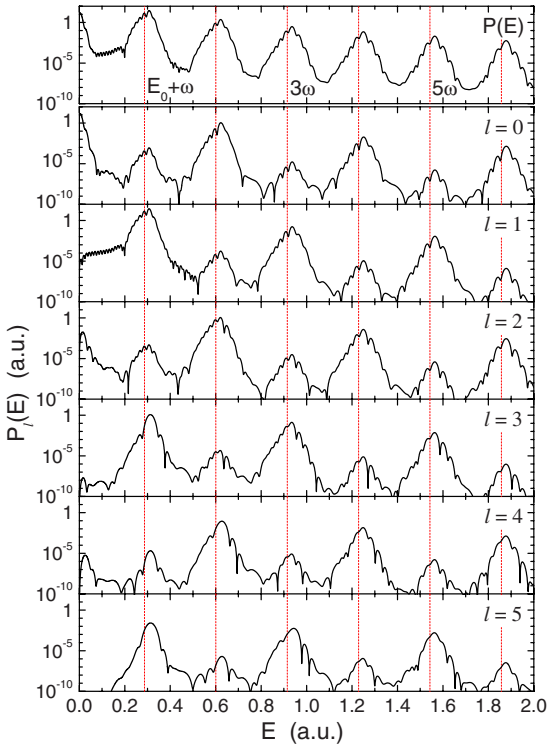

FIG. 1. (Color online) Partial-wave $P_l(E)$ and total $P(E)$ energy distributions of photodetached electrons for $F_0=0.5$, $\omega=\pi/10$, and $T=500$. Vertical dotted lines indicate positions of multiphoton absorption energies $E=E_0+n\omega$. All panels have the same scale.

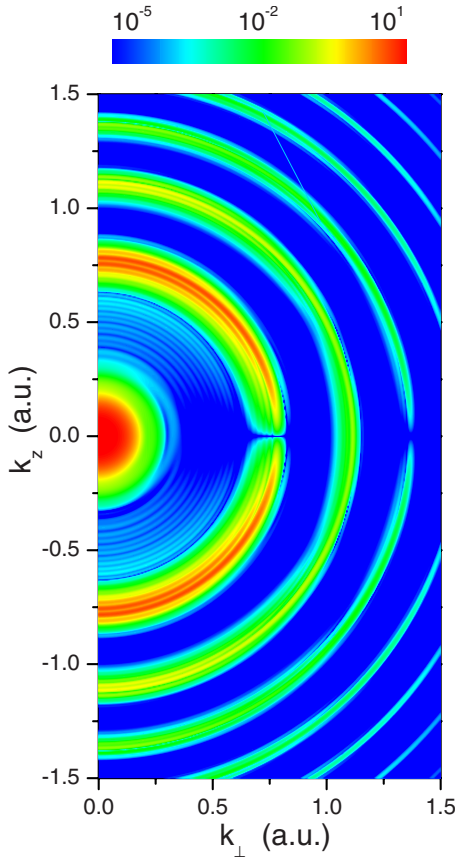

FIG. 2. (Color online) A map of the 3D electron momentum distribution $P(\mathbf{k})$ for the same laser pulse as in Fig. 1 and Table I.

tion $P(\mathbf{k})$ depends only on k_z and $k_\perp = \sqrt{k_x^2 + k_y^2}$. The ATI peaks are seen as bright rings in the figure. The odd-order rings seem to be broken at $k_z = 0$ because the dominant contribution to them comes from partial waves with odd l. One can notice finer rings in the momentum distribution between a maximum at $k = 0$ and the first ATI ring, which can be also seen as rapid oscillations in the low-energy part of the spectrum $P_1(E)$ in Fig. 1. The energy spacing between these rings is $2\pi/T$, so they result from a finite spectral width of the pulse.

The results shown in Figs. 1 and 2 contain a lot of interesting physics. However, their detailed analysis would go beyond the present illustrative purposes. Here, we focus on only one feature which can be seen in Figs. 1 and 2 as an oscillating substructure of ATI peaks. The total energy spectrum $P(E)$ shown in Fig. 1 is reproduced in linear scale in the energy range around the first ATI peak by solid lines in Figs. 3–5. The oscillating substructure of the first ATI peak is seen much more clearly in these figures. This substructure results from the interference of wave packets created in the rising and falling parts of the laser pulse. The appearance of more than one (two) temporarily separated electron wave packets in the photodetachment dynamics of H^- for similar parameters of the laser pulse, which is related to the present effect, was first detected in the calculations reported in [36]. A detailed discussion and interpretation of the interference mechanism responsible for the appearance of oscillations in

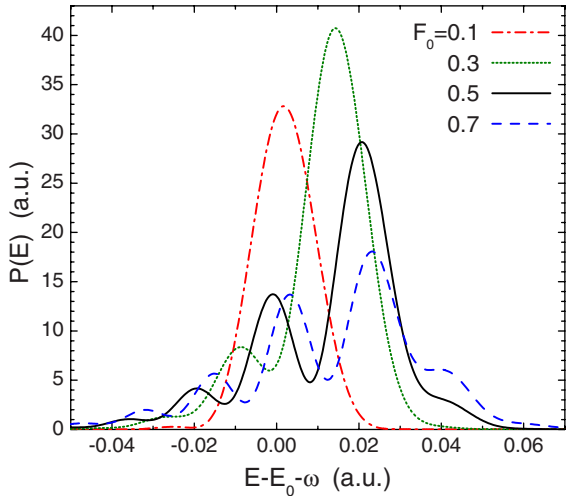

FIG. 3. (Color online) The first ATI peak for pulses with $\omega = \pi/10$, $T = 500$, and several values of F_0 which correspond to $\alpha \approx 1$, 3, 5, and 7, respectively.

the spectrum and its approximate quantitative description in terms of an adiabatic version of the high-frequency Floquet theory [40,46] in the 1D case was given in [21]. The present calculations demonstrate that the interference effect found in [21] reveals itself in the 3D case as well. The physical explanation of the effect remains the same, so we shall not repeat it here and refer the interested reader to Ref. [21]. In the rest of this section, we discuss what happens with the shape of the first ATI peak as the parameters of the laser pulse are varied around their values in the reference pulse and thus determine the range of the parameters where the effect could be observed.

First, we discuss the dependence on the amplitude F_0 of the pulse. Let us keep $\omega = \pi/10$ and $T = 500$ fixed, as in the reference pulse, and vary F_0. The energy spectra of the photodetached electrons in the region of the first ATI peak are shown in Fig. 3. The key parameter for understanding these results is $\alpha = F_0/\omega^2$ [21]. For small F_0, and hence small α, the photodetachment rate reaches its maximum only once—at the maximum of the pulse. In this case the ATI peak has a simple bell-like shape similar to that in the perturbative regime without any pronounced substructure. As F_0 grows and α becomes larger than the first critical value α_{c1}, the photodetachment rate acquires two maxima, one in the rising and another in the falling parts of the pulse. In this case two electron wave packets are formed whose interference produces an oscillating substructure of the ATI peak. As can be seen from Fig. 3, in the present case the substructure appears for $F_0 = 0.3$; hence, α_{c1} is approximately 3. As F_0 grows further, α may become larger than the second critical value α_{c2}. Then two pairs of wave packets are formed and the ATI peak consists of two separated in energy subpeaks, each having an interference substructure [21]. Thus we can conclude that a necessary condition for the observation of the effect in the present system is $\alpha > 3$.

Second, we discuss the dependence on the duration T of the pulse. Let us keep $F_0 = 0.5$ and $\omega = \pi/10$ fixed, as in the reference pulse, and vary T. The results are shown in Fig. 4.

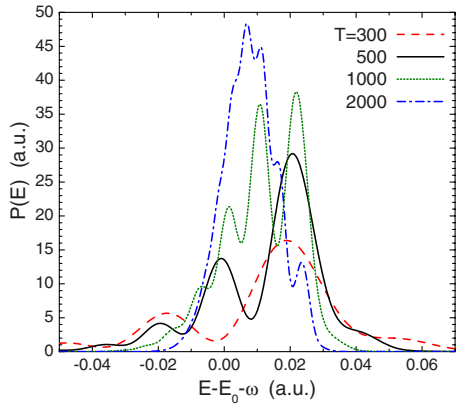

FIG. 4. (Color online) The first ATI peak for pulses with $F_0=0.5$, $\omega=\pi/10$, and several values of T which correspond to $n_{oc}=15$, 25, 50, and 100, respectively.

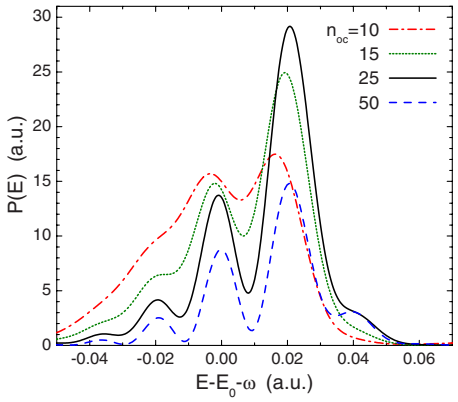

FIG. 5. (Color online) The first ATI peak for pulses with $T=500$ and several combinations of ω and F_0 such that $\alpha=F_0/\omega^2=50/\pi^2$ is kept fixed. The corresponding values of $n_{oc}=\omega T/2\pi$ are indicated.

The effect of T on the interference substructure is twofold [21]. On the one hand, the interference phase is proportional to T, with a coefficient dependent on the energy E of the ejected electron. Thus the pulse should be sufficiently long to have at least a few interference fringes within the width of the ATI peak. On the other hand, the two interfering electron wave packets must have comparable amplitudes to have a good contrast of the interference fringes. Therefore the pulse should not be too long; otherwise, almost complete photodetachment occurs in the rising part of the pulse and the second wave packet will have a negligible amplitude. This consideration is confirmed by the results in Fig. 4. As can be seen from the figure, the interference substructure in the present system is clearly visible for T in the interval from a few hundred to about 2000.

Finally, we discuss the dependence on the frequency ω of the pulse. The validity of the argumentation developed in [21] requires $\omega \gg |E_0|$. At the same time, we have seen that for the observation of the effect condition $\alpha > 3$ must be satisfied. Thus for a fixed F_0 there is an interval of ω where the effect could be observed. In order to illustrate a decisive role of the parameter α, in the calculations we varied ω simultaneously with F_0 in such a way that α is kept fixed. Let us keep $T=500$ and $\alpha=50/\pi^2$ fixed and equal to their values in the reference pulse. The results are shown in Fig. 5. As ω grows, the contrast of interference fringes improves, but their number and positions, which according to [21] depend only on T and α, do not change. As follows from the figure, the effect becomes observable for $\omega > \pi/25$, which is about 5 times larger than $|E_0|$.

Summarizing, the calculations show that the parameters of the laser pulse favorable for the observation of the interference effect found in [21] are compatible with characteristics of modern lasers. An important question is whether the one-electron approximation remains valid for pulses in this range of parameters.

V. CONCLUSIONS

In this work, the Siegert-state expansion approach, originally developed in [19] for the s-wave case and then extended in [20] to the whole-axis problem, is further extended to the full three-dimensional case. A complete formulation of the approach is given, including the derivation of coupled equations defining time evolution of the coefficients in the expansion of the solution to the time-dependent Schrödinger equation in terms of partial-wave Siegert states and expressing physical observables (probabilities of transitions to discrete states and the momentum distribution of ejected particles) in terms of these coefficients. The approach is implemented in terms of Siegert pseudostates [7] and illustrated by calculations of the photodetachment of H^- by strong high-frequency laser pulses. The present calculations show that the interference effect found recently in the 1D case [21] reveals itself in the 3D case as well and hence could be observed experimentally.

The main computational advantage of the Siegert-state expansion approach over other time-dependent close-coupling schemes in atomic physics is that it enables one to treat transitions to the continuum on an equal footing with and as easily as transitions between discrete states. Another advantage is a very limited size of the box to be considered in the calculations. This was demonstrated by calculations reported in [19–21] and in the present work. An interesting question is whether this approach can be implemented in a more conventional way—i.e., in the laboratory frame using length or velocity forms of the laser-atom interaction. This would, e.g., simplify the calculation of the coupling matrix in Eqs. (46a). The problem is that in the laboratory frame the interaction does not vanish at large distances from the atom, which violates conditions (3). One can argue that in reality a laser beam always has a finite width, so conditions (3) are formally satisfied. But this width usually exceeds by many orders of magnitude the size of an atom. A more plausible argument is that the physically important interaction region is in fact restricted by the maximum departure of ionized and then rescattered electrons from the atom. Thus one can expect convergence of the results obtained in the laboratory frame as the size of the box becomes larger than that of the interaction region. This is preliminary confirmed by comparison of the results of calculations for the same system in the

laboratory [20] and KH [21] frames. More careful analysis in this direction is needed.

An even more important virtue of the present approach is that it provides a mathematical framework suitable for developing the adiabatic approximation for transitions to the continuum [22]. A generalization of the formalism and results of [22] to the three-dimensional case is the next goal in the development of the theory.

ACKNOWLEDGMENT

A financial support from the Russian Science Support Foundation is gratefully acknowledged.

[1] A. J. F. Siegert, Phys. Rev. **56**, 750 (1939).
[2] O. I. Tolstikhin, V. N. Ostrovsky, and H. Nakamura, Phys. Rev. Lett. **79**, 2026 (1997).
[3] O. I. Tolstikhin, V. N. Ostrovsky, and H. Nakamura, Phys. Rev. A **58**, 2077 (1998).
[4] G. V. Sitnikov and O. I. Tolstikhin, Phys. Rev. A **67**, 032714 (2003).
[5] K. Toyota, T. Morishita, and S. Watanabe, Phys. Rev. A **72**, 062718 (2005).
[6] R. Santra, J. M. Shainline, and C. H. Greene, Phys. Rev. A **71**, 032703 (2005).
[7] P. A. Batishchev and O. I. Tolstikhin, Phys. Rev. A **75**, 062704 (2007).
[8] S. Yoshida, S. Watanabe, C. O. Reinhold, and J. Burgdörfer, Phys. Rev. A **60**, 1113 (1999).
[9] O. I. Tolstikhin, I. Yu. Tolstikhina, and C. Namba, Phys. Rev. A **60**, 4673 (1999).
[10] O. I. Tolstikhin, V. N. Ostrovsky, and H. Nakamura, Phys. Rev. A **63**, 042707 (2001).
[11] S. Tanabe, S. Watanabe, N. Sato, M. Matsuzawa, S. Yoshida, C. O. Reinhold, and J. Burgdörfer, Phys. Rev. A **63**, 052721 (2001).
[12] E. L. Hamilton and C. H. Greene, Phys. Rev. Lett. **89**, 263003 (2002).
[13] K. Toyota and S. Watanabe, Phys. Rev. A **68**, 062504 (2003).
[14] V. Kokoouline and C. H. Greene, Phys. Rev. Lett. **90**, 133201 (2003); V. Kokoouline and C. H. Greene, Phys. Rev. A **68**, 012703 (2003); V. Kokoouline and C. H. Greene, *ibid.* **69**, 032711 (2004).
[15] Å. Larson, S. Tonzani, R. Santra, and C. H. Greene, J. Phys.: Conf. Ser. **4**, 148 (2005).
[16] G. V. Sitnikov and O. I. Tolstikhin, Phys. Rev. A **71**, 022708 (2005).
[17] V. N. Ostrovsky and N. Elander, Phys. Rev. A **71**, 052707 (2005); V. N. Ostrovsky and N. Elander, Chem. Phys. Lett. **411**, 155 (2005).
[18] R. Čurík and C. H. Greene, Phys. Rev. Lett. **98**, 173201 (2007).
[19] O. I. Tolstikhin, Phys. Rev. A **73**, 062705 (2006).
[20] O. I. Tolstikhin, Phys. Rev. A **74**, 042719 (2006).
[21] K. Toyota, O. I. Tolstikhin, T. Morishita, and S. Watanabe, Phys. Rev. A **76**, 043418 (2007).
[22] O. I. Tolstikhin, preceding paper, Phys. Rev. A **77**, 032711 (2008).
[23] R. G. Newton, *Scattering Theory of Waves and Particles* (Springer-Verlag, New York, 1982).
[24] *Handbook of Mathematical Functions*, edited by M. Abramowitz and I. A. Stegun (Dover, New York, 1972).
[25] E. Grosswald, *Bessel Polynomials*, Lecture Notes in Mathematics, Vol. 698 (Springer-Verlag, New York, 1978).
[26] V. A. Baskakov and A. V. Popov, Wave Motion **14**, 123 (1991).
[27] K. B. Oldham and J. Spanier, *The Fractional Calculus; Theory and Applications of Differentiation and Integration to Arbitrary Order* (Academic Press, New York, 1974).
[28] K. S. Miller and B. Ross, *An Introduction to the Fractional Calculus and Fractional Differential Equations* (Wiley, New York, 1993).
[29] I. Podlubny, *Fractional Differential Equations* (Academic Press, San Diego, 1999).
[30] H. A. Kramers, *Collected Scientific papers* (North-Holland, Amsterdam, 1956), p. 272.
[31] W. C. Henneberger, Phys. Rev. Lett. **21**, 838 (1968).
[32] N. L. Manakov, M. V. Frolov, B. Borca, and A. F. Starace, J. Phys. B **36**, R49 (2003).
[33] D. Dimitrovski and E. A. Solov'ev, J. Phys. B **39**, 895 (2006); C. Arendt, D. Dimitrovski, and J. S. Briggs, Phys. Rev. A **76**, 023423 (2007).
[34] R. Shakeshaft and X. Tang, Phys. Rev. A **36**, 3193 (1987).
[35] C. Laughlin and Shih-I Chu, Phys. Rev. A **48**, 4654 (1993).
[36] A. M. Popov, O. V. Tikhonova, and E. A. Volkova, Laser Phys. **5**, 1184 (1995).
[37] K. Krajewska, I. I. Fabrikant, and A. F. Starace, Phys. Rev. A **74**, 053407 (2006).
[38] A. M. Frolov, J. Phys. B **26**, L845 (1993).
[39] C. Schwartz, Phys. Rev. **124**, 1468 (1961).
[40] M. Gavrila, J. Phys. B **35**, R147 (2002).
[41] A. M. Popov, O. V. Tikhonova, and E. A. Volkova, J. Phys. B **36**, R125 (2003).
[42] D. O. Harris, G. G. Engerholm, and W. D. Gwinn, J. Chem. Phys. **43**, 1515 (1965).
[43] A. S. Dickinson and P. R. Certain, J. Chem. Phys. **49**, 4209 (1968).
[44] J. C. Light, I. P. Hamilton, and J. V. Lill, J. Chem. Phys. **82**, 1400 (1985).
[45] P. Agostini, F. Fabre, G. Mainfray, G. Petite, and N. K. Rahman, Phys. Rev. Lett. **42**, 1127 (1979).
[46] M. Gavrila and J. Z. Kaminski, Phys. Rev. Lett. **52**, 613 (1984).